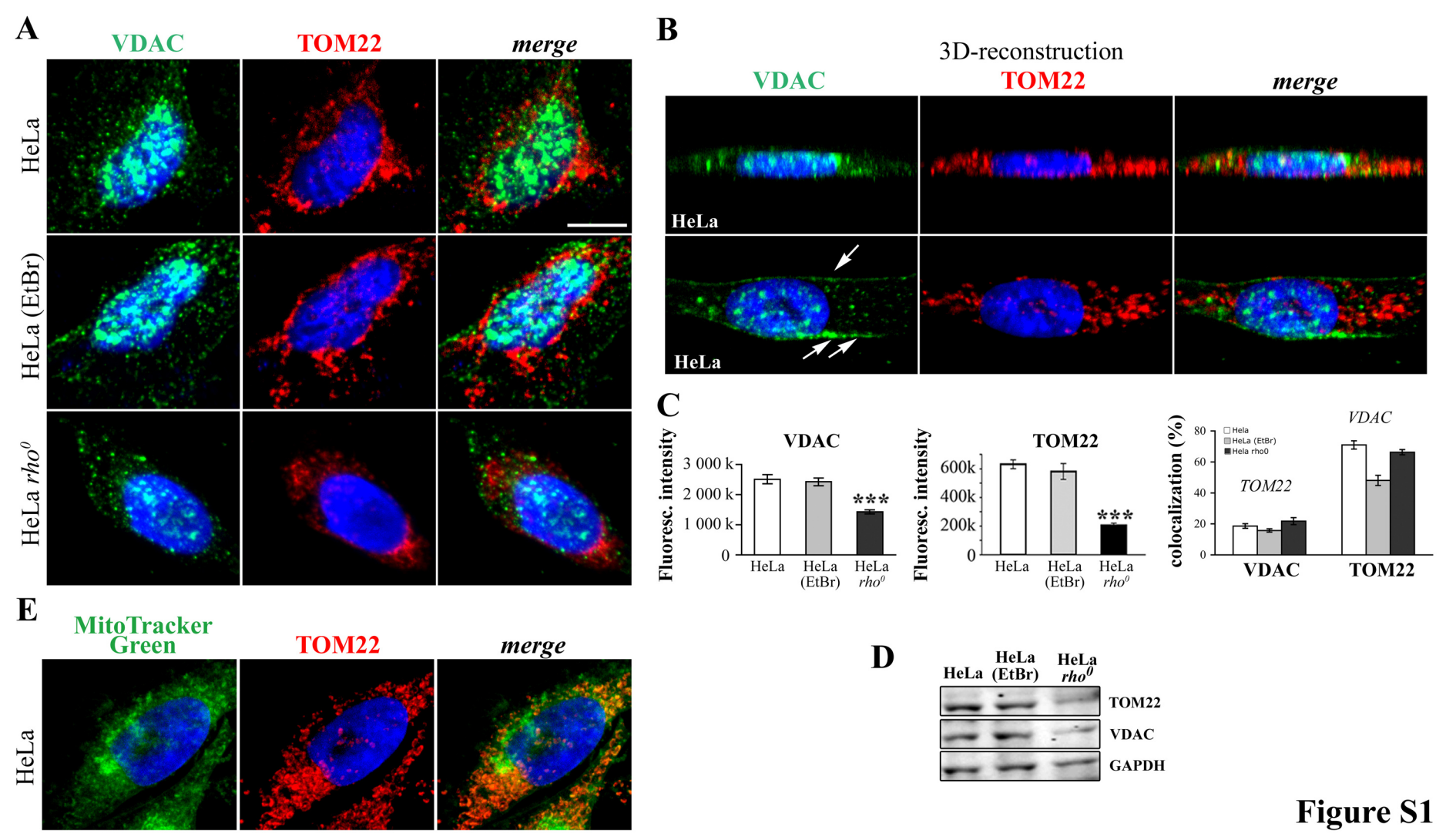
A
VDAC
TOM22
merge
HeLa
HeLa (EtBr)
HeLa rho0
B
3D-reconstruction
VDAC
TOM22
merge
HeLa
HeLa
C
VDAC
Fluoresc. intensity
3 000 k
2 000 k
1 000 k
0
***
HeLa
HeLa (EtBr)
HeLa rho0
TOM22
Fluoresc. intensity
600k
400k
200k
0
***
HeLa
HeLa (EtBr)
HeLa rho0
colocalization (%)
Hela
HeLa (EtBr)
Hela rho0
TOM22
VDAC
80
60
40
20
0
VDAC
TOM22
D
HeLa
HeLa (EtBr)
HeLa rho0
TOM22
VDAC
GAPDH
E
MitoTracker Green
TOM22
merge
HeLa

Figure S1

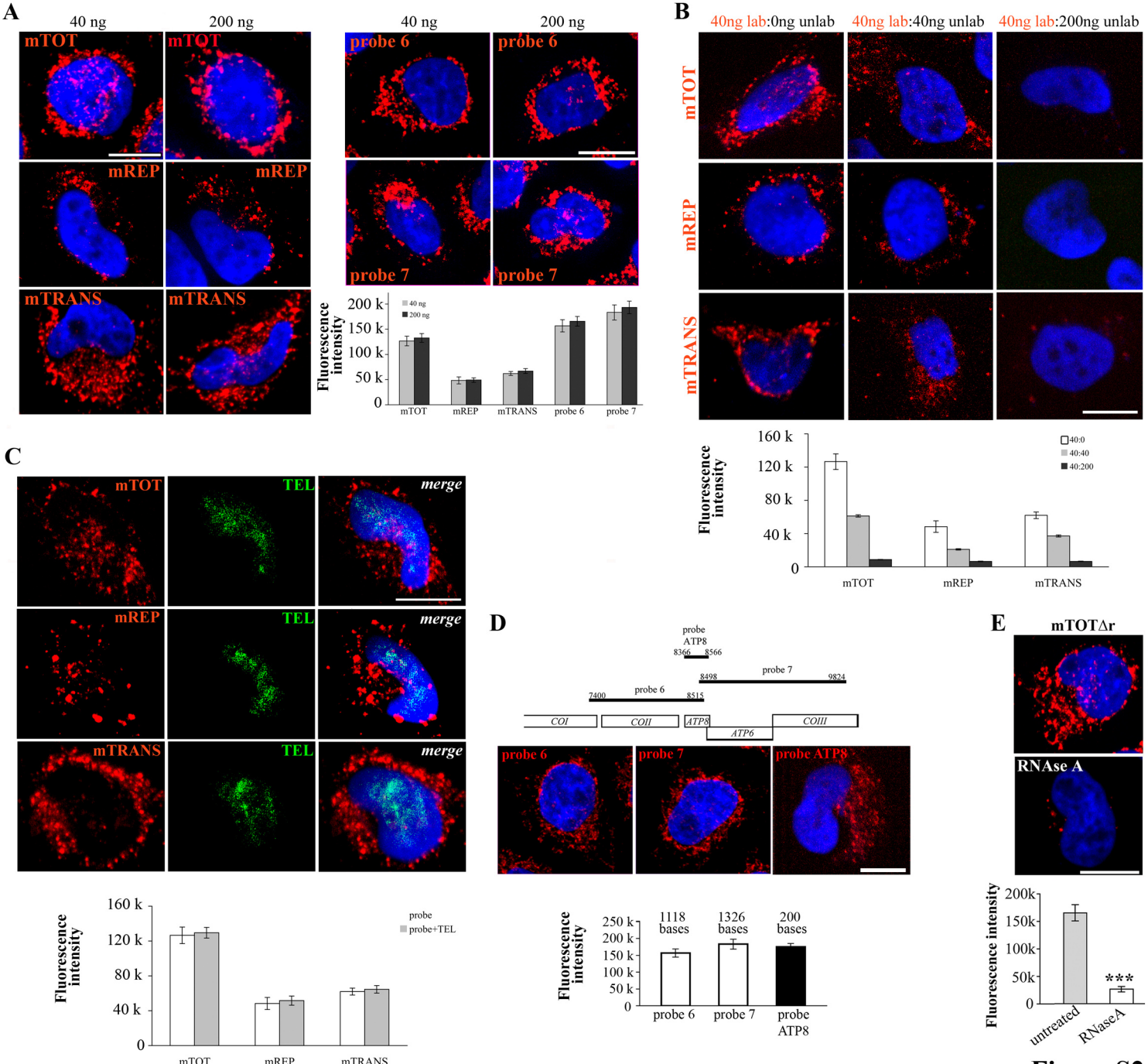
A
40 ng
200 ng
mTOT
mREP
mTRANS
probe 6
probe 7
Fluorescence intensity
200 k
150 k
100 k
50 k
0
40 ng
200 ng
mTOT
mREP
mTRANS
probe 6
probe 7
B
40ng lab:0ng unlab
40ng lab:40ng unlab
40ng lab:200ng unlab
mTOT
mREP
mTRANS
Fluorescence intensity
160 k
120 k
80 k
40 k
0
40:0
40:40
40:200
mTOT
mREP
mTRANS
C
mTOT
mREP
mTRANS
TEL
merge
Fluorescence intensity
160 k
120 k
80 k
40 k
0
probe
probe+TEL
mTOT
mREP
mTRANS
D
probe
ATP8
8366
8566
probe 7
8498
9824
probe 6
7400
8515
COI
COII
ATP8
ATP6
COIII
probe 6
probe 7
probe ATP8
Fluorescence intensity
250 k
200 k
150 k
100 k
50 k
0
1118 bases
1326 bases
200 bases
probe 6
probe 7
probe ATP8
E
mTOTΔr
RNAse A
Fluorescence intensity
200k
150k
100k
50k
0
***
untreated
RNaseA

Figure S2

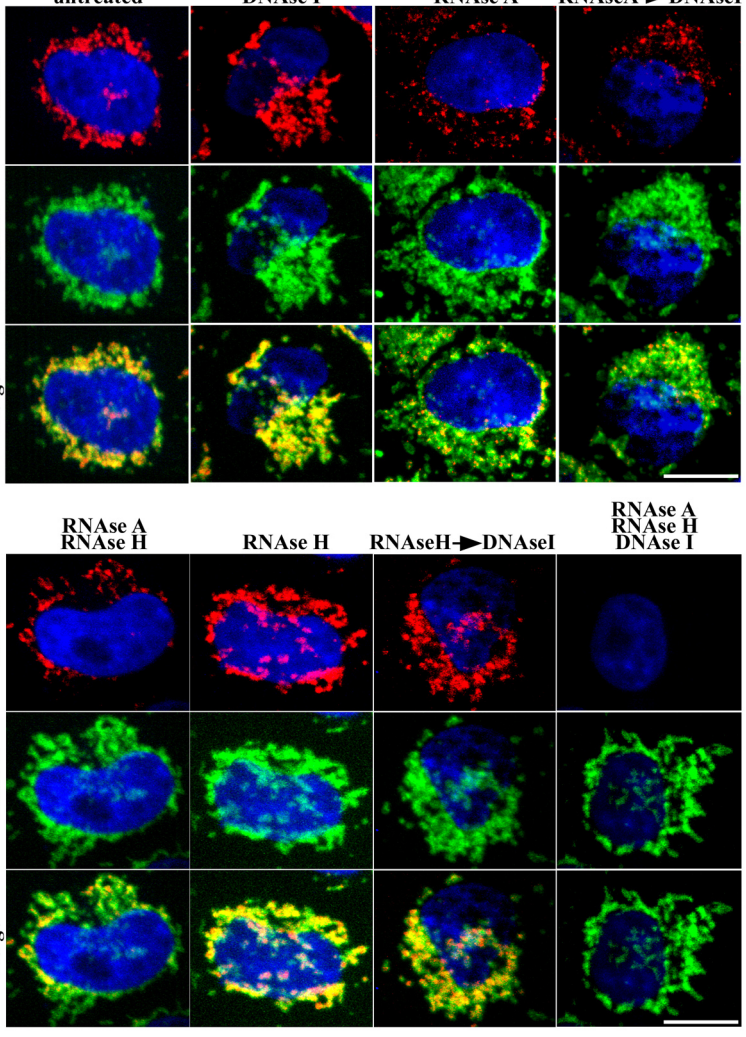
untreated
DNAse I
RNAse A
RNAseA➔DNAseI
mTOT
TOM22
merge
RNAse A
RNAse H
RNAse H
RNAseH➔DNAseI
RNAse A
RNAse H
DNAse I
mTOT
TOM22
merge

Figure S3

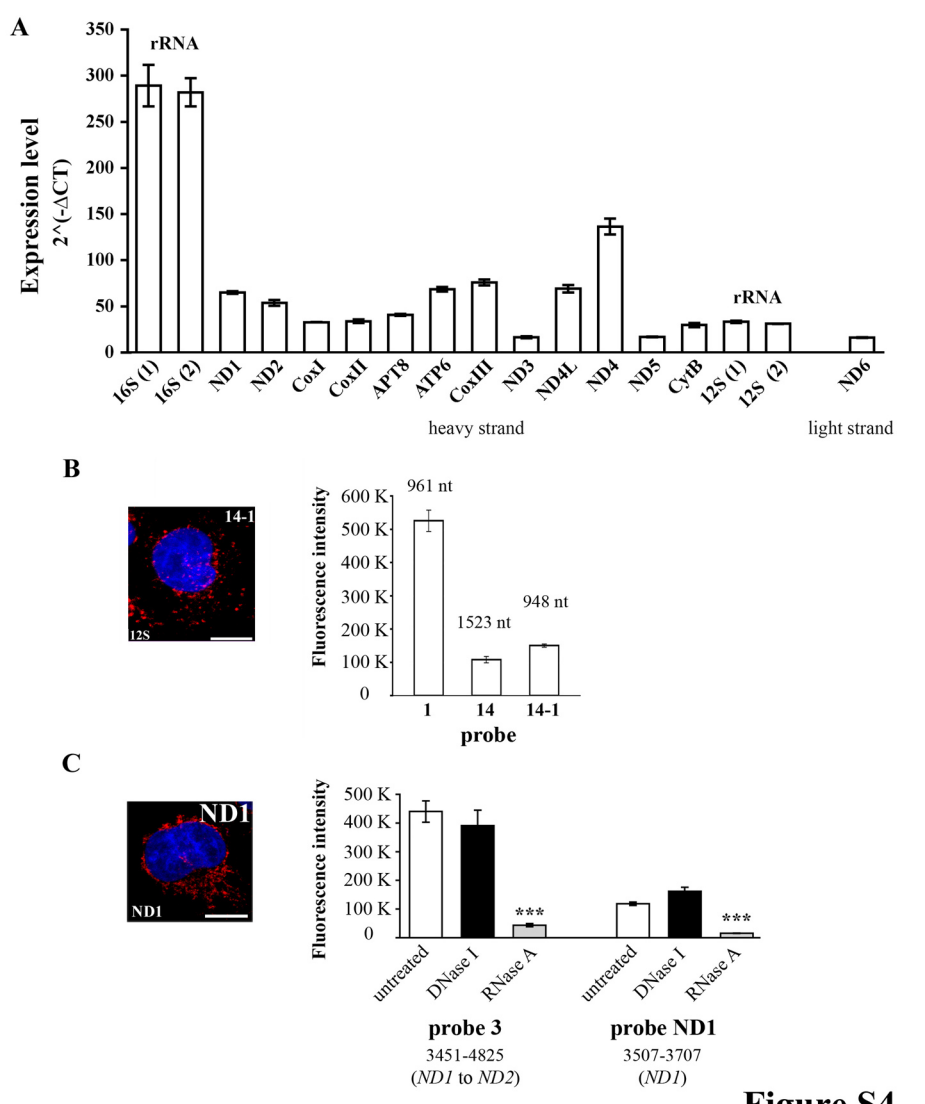
A
Expression level
2^(-ΔCT)
350
300
250
200
150
100
50
0
rRNA
rRNA
16S (1)
16S (2)
ND1
ND2
CoxI
CoxII
APT8
ATP6
CoxIII
ND3
ND4L
ND4
ND5
CytB
12S (1)
12S (2)
ND6
heavy strand
light strand
B
14-1
12S
961 nt
948 nt
1523 nt
Fluorescence intensity
600 K
500 K
400 K
300 K
200 K
100 K
0
1
14
14-1
probe
C
ND1
ND1
500 K
400 K
300 K
200 K
100 K
0
***
***
untreated
DNase I
RNase A
untreated
DNase I
RNase A
probe 3
3451-4825
(ND1 to ND2)
probe ND1
3507-3707
(ND1)

Figure S4

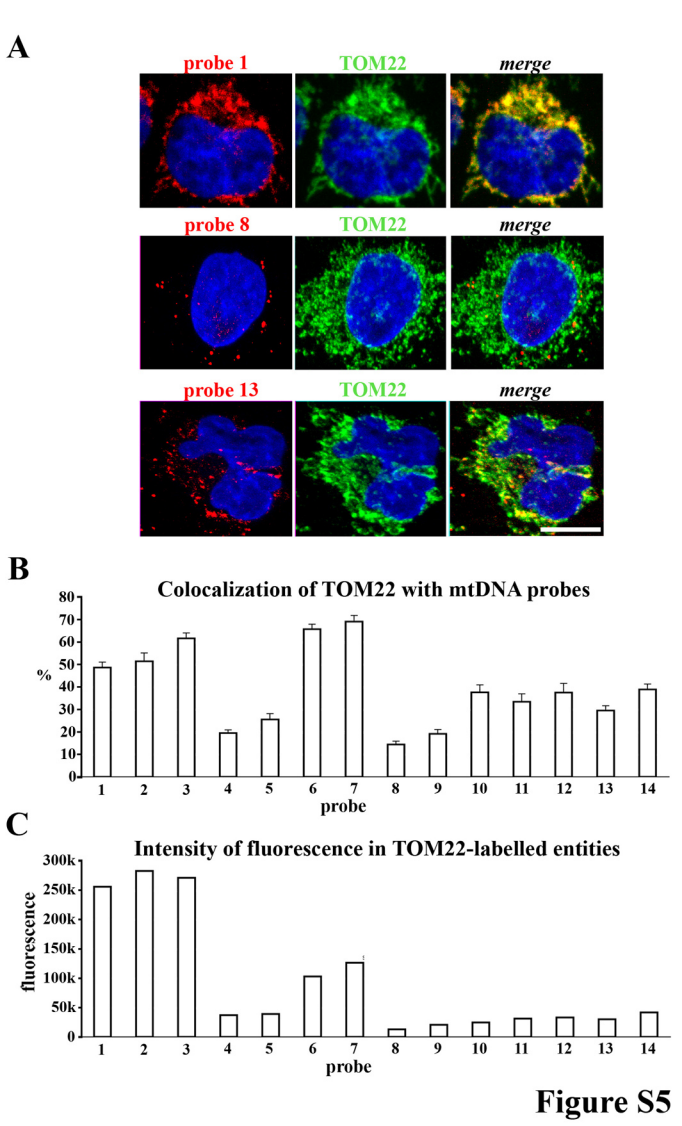
A
probe 1
TOM22
merge
probe 8
TOM22
merge
probe 13
TOM22
merge
B
Colocalization of TOM22 with mtDNA probes
%
80
70
60
50
40
30
20
10
0
1
2
3
4
5
6
7
8
9
10
11
12
13
14
probe
C
Intensity of fluorescence in TOM22-labelled entities
fluorescence
300k
250k
200k
150k
100k
50k
0
1
2
3
4
5
6
7
8
9
10
11
12
13
14
probe

Figure S5

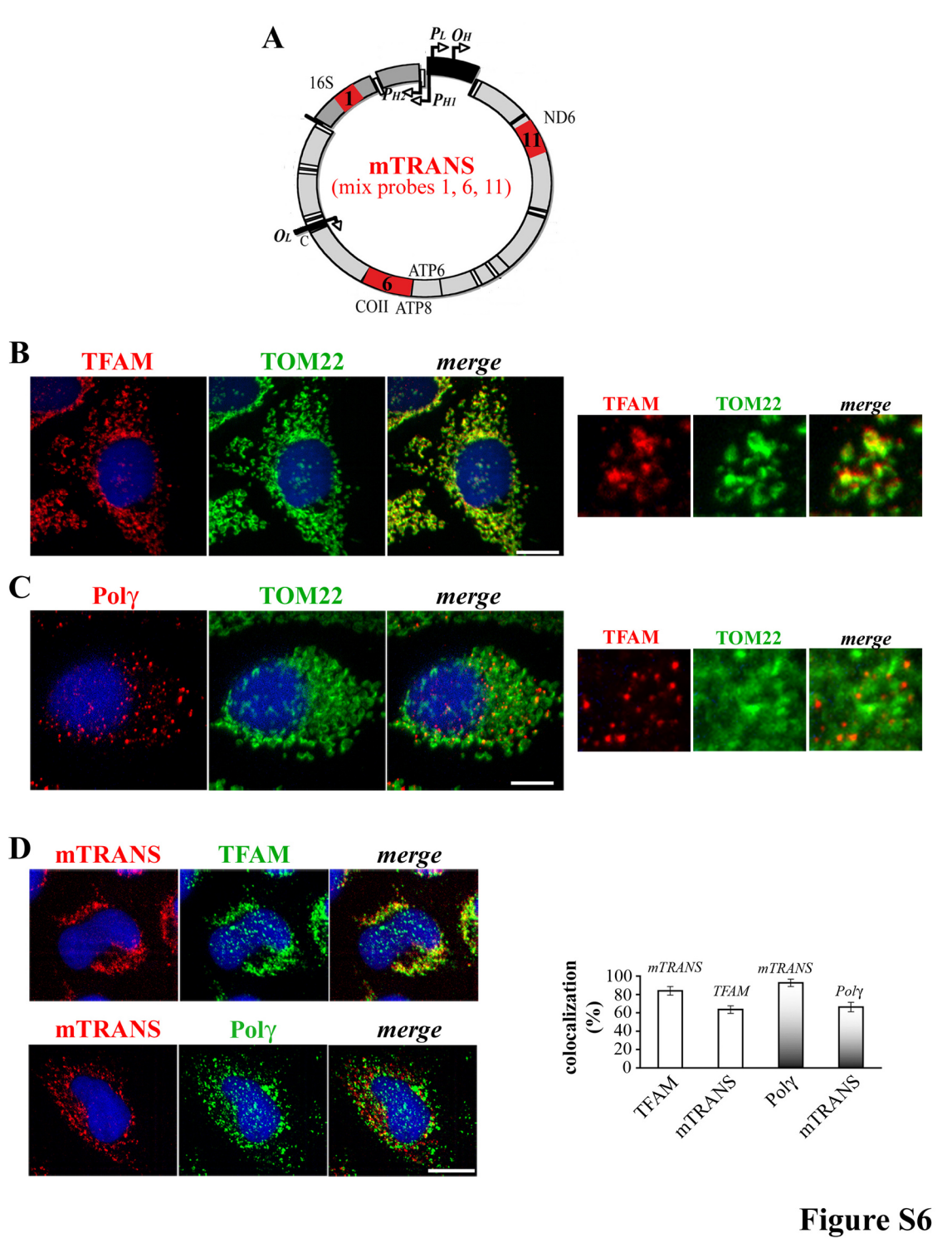
A
PL OH
16S
1
PH2
PH1
ND6
11
mTRANS
(mix probes 1, 6, 11)
OL
C
ATP6
6
COII ATP8
B
TFAM
TOM22
merge
TFAM
TOM22
merge
C
Polγ
TOM22
merge
TFAM
TOM22
merge
D
mTRANS
TFAM
merge
mTRANS
Polγ
merge
colocalization (%)
100
80
60
40
20
0
mTRANS
TFAM
mTRANS
Polγ
TFAM
mTRANS
Polγ
mTRANS

Figure S6

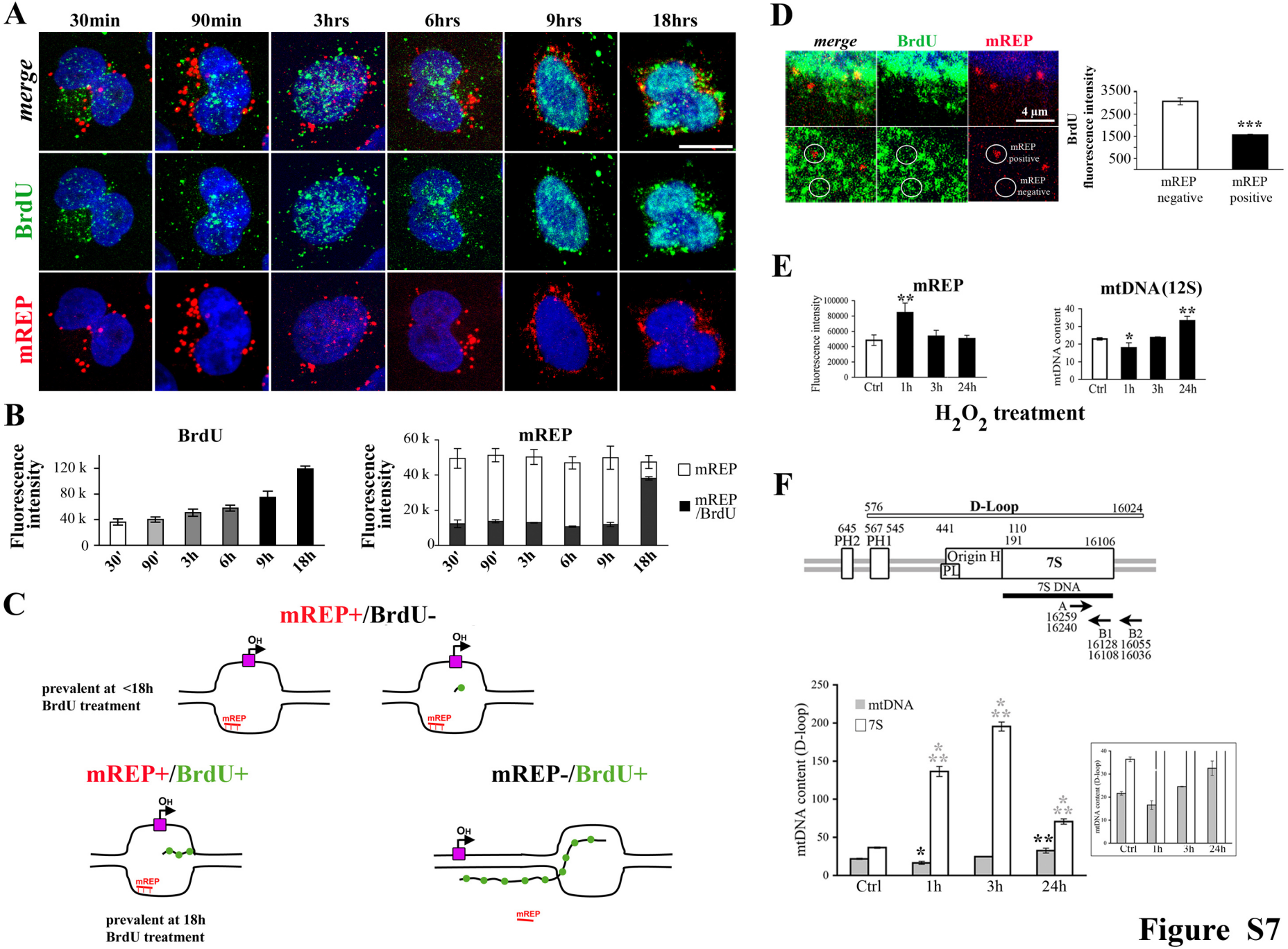
A
30min
90min
3hrs
6hrs
9hrs
18hrs
merge
BrdU
mREP
B
BrdU
Fluorescence intensity
120 k
80 k
40 k
0
30'
90'
3h
6h
9h
18h
mREP
60 k
40 k
20 k
0
mREP
/BrdU
C
mREP+/BrdU-
prevalent at <18h
BrdU treatment
OH
mREP
mREP+/BrdU+
mREP-/BrdU+
prevalent at 18h
BrdU treatment
D
merge
BrdU
mREP
4 μm
mREP positive
mREP negative
BrdU fluorescence intensity
3500
2500
1500
500
***
mREP negative
mREP positive
E
mREP
Fluorescence intensity
100000
80000
60000
40000
20000
0
**
Ctrl
1h
3h
24h
mtDNA (12S)
mtDNA content
40
30
20
10
0
*
**
H2O2 treatment
F
576
D-Loop
16024
645
PH2
567
PH1
545
441
110
191
16106
Origin H
PL
7S
7S DNA
A
16259
16240
B1
16128
16108
B2
16055
16036
mtDNA content (D-loop)
250
200
150
100
50
0
mtDNA
7S
*
**
Ctrl
1h
3h
24h

Figure S7

A

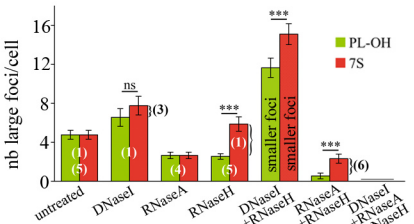

B

large foci

PL-OH	7S	
RNA/DNA	RNA	pattern (1)
-	DNA a/o RNA a/o RNA/DNA	pattern (2)
DNA	RNA a/o RNA/DNA	pattern (3)
RNA/DNA	DNA a/o RNA/DNA	pattern (4)
RNA (a/o RHR-RNA/DNA)	RNA (a/o RHR-RNA/DNA)	pattern (5)
-	DNA	pattern (6)

Figure S8

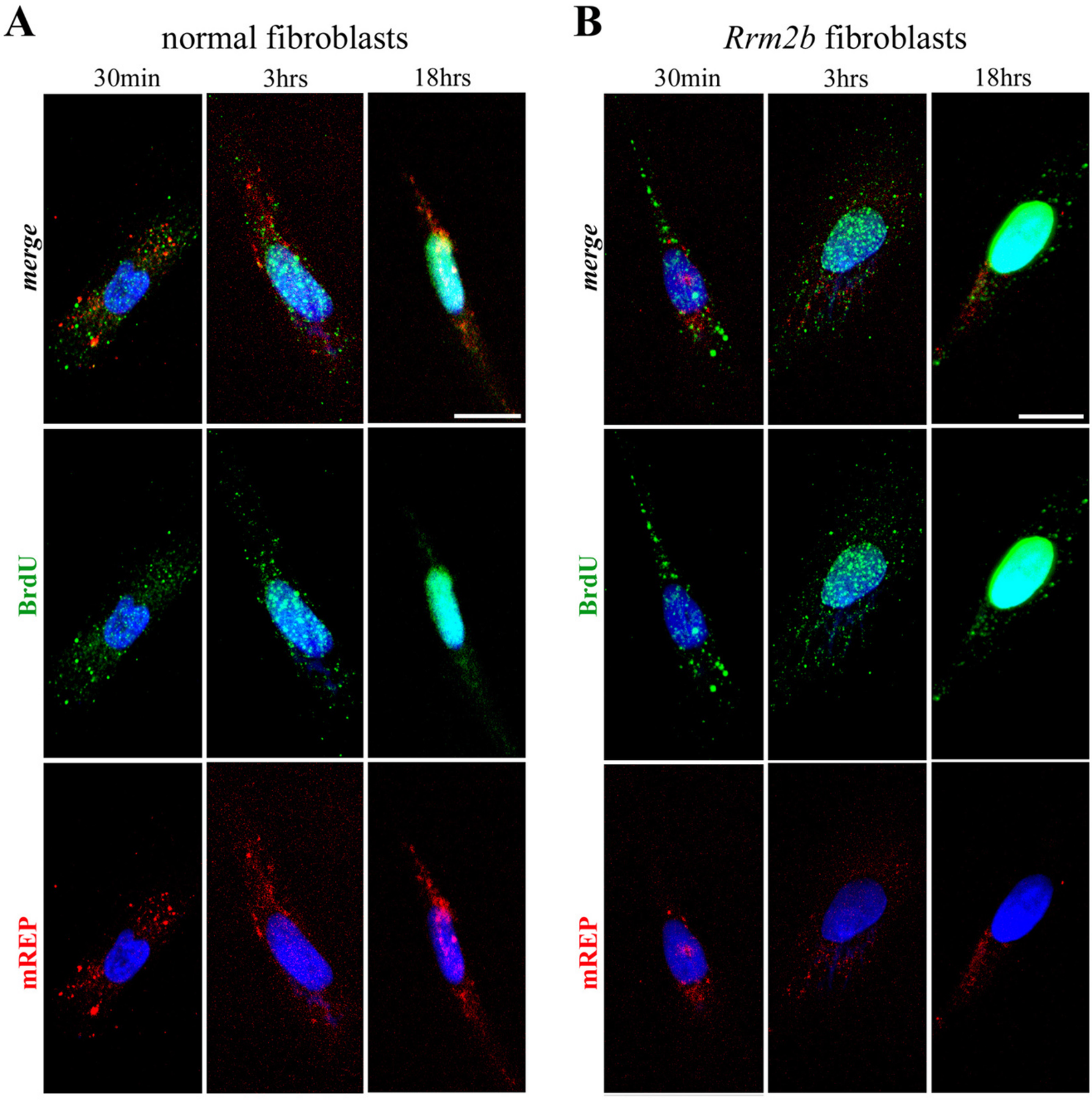
A
normal fibroblasts
30min
3hrs
18hrs
merge
BrdU
mREP
B
Rrm2b fibroblasts
30min
3hrs
18hrs
merge
BrdU
mREP

Figure S9

Supplementary Figure legends

Figure S1. Detection of the mitochondrial network in HeLa cells. (A) 3D-reconstructed HeLa cells (upper panels) immunolabeled with VDAC1/2/3 (green), TOM22 (red), and merge. Nuclei are labeleld with Hoechst (blue). Note the large VDAC (but not TOM22) signal in the correspondence of the nucleus, in agreement with several reports showing that VDACs are localized also in extramitochondrial membranes, including the plasma membrane and the endoplasmic reticulum, ER, (De Pinto et al., 2010, *FEBS Lett*. 584: 1793-1799; Mathupala and Pedersen, 2010, *Cancer Biol. Ther.* 9: 1053-1056; Elinder et al., 2005 *Cell Death Differ*. 12: 1134-1140; Shoshan-Barmatz and Israelson, 2005, *J. Membr. Biol*. 204:57-66; Bahamonde et al, 2003, *J. Biol. Chem.* 278: 33284-33289; Thinnes, 1992, *J. Bioenerg. Biomembr*. 24:71-75). The perninuclear labelling of VDAC in this panel is in agreement with its detected presence in the perinuclear ER. Different intracellular VDAC versus TOM22 labelling is also shown in HeLa cells treated for three days with EtBr to deplete the mtDNA (middle panels), and HeLa *rho*^{0} cells, which contain mitochondria but not mtDNA (lower panels). EtBr-treated Hela cells and *rho*^{0} cells are used later in this study. **(B)** Two plans of the 3D-volume rendering of a HeLa cell labelled as in panel (A). Note also the presence of VDAC (but not TOM22) at the extreme periphery of the cytoplasm (white arrows), likely in the plasma membrane. **(C)** Quantification of the fluorescence intensity of VDAC and of TOM22 (values of TOM22 are from Fig. 6B). The right panel shows colocalization of VDAC (on the X-axis) with TOM22, and of TOM22 (on the X-axis) with VDAC in untreated, EtBr-treated, and *rho*^{0} HeLa cells. A large fraction of VDAC does not colocalize with TOM22, compatibly with the localization of VDAC, but not of TOM22, in the nuclear region and in other extramitochondrial membranes (see above). Conversely, TOM22 largely colocalizes with VDAC. Note that the absence of colocalization may also be due to one of the two markers being present below the detection level. Moreover, the heterogeneity of intramitochondrial localization of VDAC versus TOM22 (VDAC1/2 are present in specific domains of the mitochondrial membrane, Neumann et al, 2010, *PMC Biophysics*, 3:4. TOM22 appears homogenously diffused in the mitochondria, Yano et al, 200, *Mol. Cell. Biol* 19: 7205-7213) may also be responsible for the absence of colocalization signal at certain positions. **(D)** Western blot of TOM22 and VDAC in untreated, EtBr-treated and *rho*^{0} HeLa cells show that each of the two proteins is present at comparable levels in untreated and EtBr-treated cells, whereas the levels drop in *rho*^{0} cells, in agreement with immunofluorescence data. **(E)** Colocalization of MitoTracker® Green FM, a green–fluorescent mitochondrial stain that selectively accumulates in the mitochondrial matrix, and TOM22. Scale bar = 10 μm.

Figure S2. mTRIP signal is specific and is not limited by probe concentration nor is affected by probe size. (A) 3D-reconstructed HeLa cells labeled with the mTOT probe (red) at saturating (200 ng) and at regular concentrations (40 ng), upper panels. Additional four probes used in this study (mREP, mTRANS, probes 6 and 7) were tested at regular and saturating concentrations. The graphic on the right below shows the fluorescence intensity quantification. For each probe, no differences between the two conditions (t-test). These data indicate that the labelling of a subset of mitochondria by mTRIP is not due to limited concentrations of the probe. **(B)** Competition experiments between 40 ng of labelled probe ("lab", red) and increasing concentrations (0 ng, 40 ng and 200 ng) of unlabelled ("unlab", black) probe. Probes mTOT, mREP and mTRANS were tested. Below, fluorescence intensity quantification shows that, for each probe, the labelling is specific (reduction of the signal in the presence of increasing amounts of unlabelled probe). **(C)** Labelling (red) of probes mTOT, mREP and mTRANS is unaffected by the presence of probe TEL (5'TTAGGG repeats, green) that recognizes nuclear telomeric sequences. Below, fluorescence intensity quantification. T-test, no differences between the samples. **(D)** mTRIP signal is not affected by the probe size. Upper panel: schematic representation of the position of the probes (with the mitochondrial coordinates, see also Table S2) and of the genes present in the region tested; tRNAs are not represented. Mitochondrial coordinates according to MITOMAP (http://www.mitomap.org/MITOMAP). Middle panels: mTRIP labelling of HeLa cells with the indicated probes (red). Lower panel, fluorescence intensity quantification of 3D-reconstructed cells. The probe size is indicated on top. T-test, no differences between the samples. These data indicate that the probe size (200-1300 nt in length) does not affect the efficiency of FISH labelling. **(E)** 3D-reconstructed HeLa cells labeled with probe mTOTΔr, that consists in mTOT without probes that cover the mt ribosomal genes (probes 1, 2 and 14), untreated, and treated with RNaseA. Lower panel: fluorescence intensity quantification. t-test, compared to untreated cells. The intensity of labelling in the absence of rDNA probes is at least as high as with the probe mTOT (fluorescence intensity about 130k for mTOT, from in Fig. 1H), indicating that mTRIP labels mitochondrial mRNAs even in the presence of large amounts of rRNAs. Scale bars= 10 µm. Nuclei (blue) are labelled with Hoechst.

Figure S3. Mitochondrial network and mTRIP labelling in the presence and in the absence of nucleases. 3D-reconstructed HeLa cells labelled with probe mTOT (red), TOM22 immunolabelled (green), and merge, with or without nuclease(s) treatment (specified on the top of each panel; arrow indicates that second nuclease was added after 1h incubation with

first nuclease). mTOT labelling alone (in another set of cells) is shown in Fig. 1G. Scale bars= 10 μm.

Figure S4. Expression levels of the individual mitochondrial genes by RT-qPCR and additional analysis of specific *loci*. (A) Real-time quantitative PCR of individual mitochondrial genes in HeLa cells. 16S and 12S were analyzed with two independent sets of primers, (1) and (2). Expression level profiles of the mitochondrial genes are compatible with those observed by mTRIP analysis. Note that RT-qPCR detects transcripts of the entire mitochondrial and cellular populations whereas mTRIP reveals RNAs in a fraction of mitochondria and at the single-cell level. **(B)** Left panel: 3D-reconstructed HeLa cell with probe 14-1 that labels the 12S region (Table S2), scale bar= 10 μm. Right panel: fluorescence intensity quantification of probe 14-1. Data for probes 14 that labels 12S, and for probe 1 that labels 16S are from Fig. 2B and are shown for comparison. The size of the probes, in nucleotides, is indicated on the top of the column. These data show low mTRIP signal for *12S* with two independent sets of probes (14 and 14-1). Data from panels A-B are in agreement with the observation that, in spite mitochondrial RNAs are transcribed from a single molecule (essentially rRNAs from promoter P_{H1}, and mRNAs of the H-strand from promoter P_{H2} (Montoya et al, 1983, *Cell* 34: 151-9), different levels of individual RNAs are detected, compatibly with the turnover of the single transcripts (Gelfand and Attardi, 1981, *Mol. Cell. Biol.* 1: 497-511; Piechota et al., 2006, *Acta Biochim. Pol.* 53: 157-68). This is the case not only for mRNAs but also for 12S rRNA, which is detected here at lower levels than 16S rRNA (FISH and RT-qPCR experiments, for a total of seven loci examined), although similar levels of the two rRNAs were observed in vitro (Gelfand and Attardi, 1981, *cited*) and in vivo (Mercer et al., 2011, *Cell* 146: 645-658). Lower levels of 12S than 16S RNAs were nevertheless observed in several primary cells (Ninomiya and Ichinose, 2007, *PLoS One 2*: e1241; Welle et al., 1999, *Genome Res*. 9: 506-13), and the two rRNAs also appear differently sensitive to methylation (Cotney et al., 2009, *Hum. Mol. Genet*. 18: 2670-82; Metodiev et al., 2009, *Cell. Metab.* 9: 386-97) and to specific mitochondrial factors including ribosomes (Hyvarinen et al., 2010, *BMC Mol. Biol.* 11: 72; Smits et al., 2011, *Eur. J. Hum. Genet.*, 19: 394-9), indicating that lower levels of 12S versus 16S RNA detected with our analysis are compatible with reported physiological situations. **(C)** Left panel: 3D-reconstructed HeLa cell labelled with probe ND1, which recognizes a portion of the *ND1* gene (Table S2). Right panel: fluorescence intensity quantification of probe ND1 (and of probe 3, data from Fig. 2B, used as comparison) in presence and absence of nucleases. For each probe the coordinates in

the mitochondrial genome, and the target genes (in parenthesis), are indicated below. T-test, compared to untreated cells. Scale bars= 10 μm. The transcript levels of *ND1* (panel A) are compatible with the intensity of the mTRIP signal with the specific probe ND1 but not with probe 3, which labels additional genes, and probably also unterminated rRNA transcripts (see Fig. 3).

Figure S5. Colocalization of mTRIP labelling with mitochondria. (**A**) 3D-reconstructed HeLa cells labelled with the indicated mtDNA probe (red) and anti-TOM22 (green). Probes 1 (upper panels), 8 (middle panels), and 13 (lower panels) show high, low and intermediate colocalization levels with TOM22, respectively. **(B)** Percentage (p) of colabelling with mTRIP probes and anti-TOM22; n=30 cells; three independent experiments. A larger fraction of mitochondria carries *16S* RNA (probes 1-2), and *COII*, *ATP6*, *ATP8*, *COIII* RNAs (probes 6-7), than of the other mitochondrial transcripts. *COII* and *ATP6/8* have a longer half-live than the other transcripts in HeLa cells (Piechota et al., 2006, *Acta Biochim Pol* 53, 157-68). Probe 3 also shows high colocalization levels, but data in Fig. 3A,B indicate that this probe may also label unterminated rRNA transcripts. **(C)** Intensity of fluorescence in TOM22-labelled entities, calculated for each probe by multiplying the intensity of fluorescence of the probe (fi) by the percentage (p) of mTRIP labelled mitochondria (= fi x p). Each value indicates the relative amount of transcripts carried by the TOM22-labelled mitochondrial structures. Data in panels B and C indicate that not only *16S* RNA is present in a larger proportion of the mitochondrial population than are the other transcripts, but also that labelled mitochondria carry larger amounts of this than of the other transcripts. Conversely, the remaining transcripts are present in a small proportion of the mitochondrial population where they are also present in minor amounts. An intermediary situation was observed for the region of the mitochondrial genome that contains *COII* to *COIII* RNAs (probes 6-7), that are present in a large portion of mitochondria but in small amounts therein. Thus, 16S rRNA labels the large majority of mitochondria, and with an elevated signal per unit, whereas the other probes mainly identify distinct and in several cases minor mitochondrial fractions.

Figure S6. Immunofluorescence of nucleoid markers TFAM and Polγ with the mitochondrial marker TOM22. (A) Schematic representation of the position of probe mTRANS (mix of probes 1, 6 and 11), in red, on the human mitochondrial genome. **(B)** Colabelling of the nucleoid marker TFAM (red) with the mitochondrial marker TOM22 (green). Nucleus is stained by Hoechst (blue). Small panels on the right (magnification) show

large colocalization between the two markers (colocalization of TOM22 with TFAM: 99.94% ± 0.02%; n= 30 cells; three independent experiments). **(C)** Colabelling of the nucleoid marker Polγ (red) with the mitochondrial marker TOM22 (green). On the right, magnifications. Polγ is detected only in a fraction of mitochondria (colocalization of TOM22 with TFAM: 24.98% ± 1.87%; n= 30 cells; three independent experiments). Scale bars= 10 μm. **(D)** mTRIP labelling with mTRANS probe (red) and either anti-TFAM (green) or anti-Polγ (green), upper and lower panels, respectively. Panel on the right shows percentages of colocalization of marker on the X-axis with the marker indicated on the top of each column; n=30, three independent experiments**.** Note that TFAM and Polγ colocalized with mTRANS by 83.89 ± 4.7 % and by 92.69 ± 4.0 %, respectively, indicating that less than one tenth of the mitochondrial nucleoids labelled with these markers did not contain transcript levels detectable by this probe mix. Conversely, mTRANS colocalized by 63.53 ± 4.1% and by 66.23 ± 5.1 % with TFAM and Polγ, respectively, indicating that about one third of the mitochondrial transcripts revealed by this probe mix was not located in nucleoids where either TFAM or Polγ are present at detectable levels. The different extents of colocalization among foci are in agreement with significantly different amounts of TFAM in nucleoids (Chen and Butow, 2005, *Nat. Rev. Genet.* 6:815-25; Shutt et al, 2010, *PNAS USA*, 107: 12133-8; Spelbrink, 2010, *IUBMB Life* 1: 19-32; Wai et al., 2008, *Nat. Genet.* 40: 1484-8), and Polγ may be present at low or undetectable levels in transcription-active nucleoids. Therefore, within the limits of resolution of mTRIP, mTRANS largely colocalizes with nucleoid markers.

Figure S7. mREP labels initiation of mtDNA replication. (A) 3D-reconstructed HeLa cells labelled with probe mREP (red) and anti-BrdU (green) at different times of exposure to 10 μm BrdU. Nuclei are labelled by Hoechst (blue). mTRIP was performed followed by BrdU immunostaining. Scale bar=10 μm. **(B)** Fluorescence intensity quantification. Left panel, BrdU; right panel, mREP (white), and proportion of mREP that colocalizes with BrdU (black); n=30, three independent experiments. Time 18h was tested in seven independent experiments. **(C)** Schematic representation of BrdU and mREP labelling patterns. mREP+ signal (red) results from hybridization of the probe to the corresponding DNA sequence (within an accessible structure). The O_H origin is schematically represented with a purple square. BrdU labelling is indicated with green spots along the newly synthesized mtDNA chain. A number of green spots below threshold results in $BrdU^-$ signal. Open mtDNA at O_H

without DNA synthesis (standby position) also results in $BrdU^-$ signal. BrdU incorporation distant from the origin O_H is not compatible with mREP labelling (inaccessible DNA structure). **(D)** Detail of 3D-reconstructed cells (2.5x magnification) labelled with mREP (red), anti-BrdU (green), and merge; nuclei are labelled by Hoechst (blue) at 18h exposure to BrdU. Two regions, proximal and distal to the nuclear surface are shown in upper and lower panels, respectively. In lower panels, circles indicate representative mREP-positive and mREP-negative areas, where BrdU labelling was also measured. On the right, fluorescence intensity measurement of BrdU labelling shows higher values in mREP-negative than in mREP-positive areas. n=300 areas, three independent experiments. Scale bar= 4μm. **(E)** mREP anticipates the increases in mtDNA content. Cells were treated with 50 μM of H_2O_2 which increases the mtDNA content (Lee et al, 2005, *Ann. NY Acad. Sci.* 1042:246-54). Fluorescence intensity quantifications of mREP, left panel; and mtDNA content estimation by qPCR (12S region), right panel. Ctrl, untreated; 1h to 24h, time in the presence of H_2O_2. n=3. T-test, compared to untreated cells. mREP labelling increase by about 70% 1h after H_2O_2 treatment, when the DNA content is low, and returned to control values 3h after treatment when the original mtDNA content was restored compatibly with the time necessary to replicate the mt genome (about 92 minutes for total mtDNA replication (Korhonen et al, 2004, *EMBO J.* 23: 2423-9)). **(F)** Upper panel, scheme of primers for the estimation of 7S DNA and mtDNA content by real-time qPCR as described (Antes et al., 2010, *Nucleic Acids Res.* 38:6466-76). 7S DNA corresponds to amplification of AB1; mtDNA corresponds amplification of AB2-AB1. Lower panel**,** cells treated with H_2O_2 as in panel E. 7S (white columns) and mtDNA (grey columns) content. The small panel on the right represents values on a scale adapted to detect the variations of mtDNA (grey columns). n=3 independent experiments. T-test, compared to untreated cells (ctrl); black stars for mtDNA, grey stars for 7S; Scale bar =10 μm.

Figure S8. Heterogeneity of nucleic acid composition in large foci at the replication origin O_H and in the 7S region (A) Enumeration of large PL-OH (green) and 7S (red) foci. The number in parenthesis represents the corresponding labelling pattern (numbered as in Fig. 5B). Pattern numbers common to PL-OH and 7S large foci are in white. Pattern numbers specific to 7S foci are in black, and in this case the proportion of events is indicated with a brace. Foci in sample treated simultaneously with DNaseI and RNAseH are smaller than in the other samples. T-test: 7S versus PL-OH foci; ns, not significant. **(B)** Scheme of nucleic acids detected in large PL-OH and 7S foci (a/o= and/or; RHR-RNA/DNA=RNaseH resistant

RNA/DNA hybrids), with the pattern number indicated on the right.

Taken together, panels A and B, as well as Fig. 5B reveal the following nucleic acid compositions. Pattern 1: about one half of large PL-OH foci are DNaseI-resistant and RNaseH-sensitive, and they essentially colocalize with foci of the downstream 7S probe. Differently from PL-OH, however, large 7S foci are essentially RNaseH-resistant. Thus, these large PL-OH and 7S foci colocalize but the former probe recognizes RNA/DNA hybrids whereas the latter recognizes RNA. Pattern 1 large foci are thus compatible with transcripts bound to the DNA template proximally to the promoter (probe PL-OH), and of single-strand RNA distally from the promoter (probe 7S). Given the direction of transcription, these nucleic acids are unlikely associated with a single transcription event. Pattern 5: most of the other half of large DNAseI-resistant PL-OH and 7S foci are RNaseH-resistant, and therefore consist of either RNAseH-resistant RNA/DNA hybrids (possibly R-loops) or of RNA. Given that about one half of PL-OH and 7S foci are also RNaseA-sensitive, and that combined RNAseA and RNAseH treatment erases most PL-OH foci, it is likely that pattern 5 corresponds to RNA at both PL-OH and 7S locations (Fig. 5D). Pattern 3: large DNaseI-resistant 7S foci and apparently DNaseI-sensitive PL-OH foci indicate accessible DNA structure at PL-OH whereas RNA (as single strand or as RNA/DNA hybrid) is present at the level of 7S. The frequency of foci in pattern 3 was not determined with significant accuracy given the low number of foci/cell, although they may account for about 15% of 7S large foci (see panel A). Pattern 4: RNaseA-resistant PL-OH and 7S foci were observed which indicate no free L-strand transcript at either position. The almost equivalent number of RNaseA-resistant and RNAseH-sensitive PL-OH foci, as well as the disappearance of foci after combined treatment with RNaseA and RNaseH, suggest that pattern 4 corresponds to RNA/DNA hybrids at PL-OH. Given the direction of transcription, the nucleic acids in pattern 4 are also unlikely associated with a single transcription event. Pattern 6: DNA in the 7S region, and no labelling in the PL-OH region. Pattern 6 reveals rare foci with exclusive DNA labelling in the 7S region, and no labelling in the PL-OH region. Interestingly, treatment with DNAseI slightly increased the number of PL-OH and 7S foci, indicating that DNA masks some RNA targets at both loci, compatibly with the presence of structured nucleic acids which also contains DNA in this region.

Figure S9. mREP and BrdU labelling in normal and *Rrm2B* fibroblasts. 3D-reconstructed fibroblasts labelled with mREP (red) and anti-BrdU (green) after 30 min, 3h and 18h treatment with BrdU. Merge images are as in Fig. 7E. Scale bar= 10 μm.

RT-qPCR primers

Probe	forward primer	reverse primer	reference
TBP	CTCACAGGTCAAAGGTTTAC	GCTGAGGTTGCAGGAATTGA	*Mercy et al. 2005. FEBS Journal 272(19):*
12S (1)	CTGCTCGCCAGAACACTACG	TGAGCAAGAGGTGGTGAGGT	*Suissa et al. 2009. PLoS Genetics 5(5):e1000474*
12S (2)	AAACTGCTCGCCAGAACACT	CATGGGCTACACCTTGACCT	*Uchuimi et al. 2010. NAR 38(16)*
16S (1)	GTATGAATGGCTCCACGAGG	GGTCTTCTCGTCTTGCTGTG	*Suissa et al. 2009. PLoS Genetics 5(5):e1000474*
16S(2)	GCTAAACCTAGCCCCAAACC	TTGGCTCTCCTTGCAAAGTT	*Uchuimi et al. 2010. NAR 38(16)*
ND1	TGGCCAACCTCCTACTCCTC	ATGGCGTCAGCGAAGGGTTG	*Suissa et al. 2009. PLoS Genetics 5(5):e1000474*
ND2	ACTGCGCTAAGCTCGCACTG	ATTATGGATGCGGTTGCTTG	*Suissa et al. 2009. PLoS Genetics 5(5):e1000474*
COI	ACCCTAGACCAAACCTACGC	TAGGCCGAGAAAGTGTTGTG	*Suissa et al. 2009. PLoS Genetics 5(5):e1000474*
COII	ACAGATGCAATTCCCGGACG	GGCATGAAACTGTGGTTTGC	*Suissa et al. 2009. PLoS Genetics 5(5):e1000474*
ATP8	ATGCCCCAACTAAATACT	TTGTGGGGGCAATGAATG	*Uchuimi et al. 2010. NAR 38(16)*
ATP6	CCCACTTCTTACCACAAGGC	GTAGGTGGCCTGCAGTAATG	*Suissa et al. 2009. PLoS Genetics 5(5):e1000474*
COIII	ACTTCCACTCCATAACGCTC	TGGCCTTGGTATGTGCTTTC	*Suissa et al. 2009. PLoS Genetics 5(5):e1000474*
ND3	CTACCATGAGCCCTACAAAC	ACTCATAGGCCAGACTTAGG	*Suissa et al. 2009. PLoS Genetics 5(5):e1000474*
ND4L	TATCGCTCACACCTCATATC	AGGCGGCAAAGACTAGTATG	*Suissa et al. 2009. PLoS Genetics 5(5):e1000474*
ND4	ACAAGCTCCATCTGCCTACG	TTATGAGAATGACTGCGCCG	*Suissa et al. 2009. PLoS Genetics 5(5):e1000474*
ND5	GGTTTCATCCTCGCCTTAGC	ACCTAATTGGGCTGATTTGC	*Suissa et al. 2009. PLoS Genetics 5(5):e1000474*
CYTB	CTCCCGTGAGGCCAAATATC	GAATCGTGTGAGGGTGGGAC	*Suissa et al. 2009. PLoS Genetics 5(5):e1000474*
ND6	ATTGGTGCTGTGGGTGAAAG	GGATCCTCCCGAATCAACCC	*Suissa et al. 2009. PLoS Genetics 5(5):e1000474*
NRF1	GGAGTGATGTCCGCACAGAA	CGCTGTTAAGCGCCATAGTG	*Savagner et al. 2003. Biochem Biophys Res Com310(3)*

qPCR primers

Probe	forward primer	reverse primer	reference
18S	GAGAAACGGCTACCACATCC	GCCTCGAAAGAGTCCTGTAT	*Suissa et al. 2009. PLoS Genetics 5(5):e1000474*
12S	GCTCGCCAGAACACTACGAG	CAGGGTTTGCTGAAGATGGC	*Parone et al. 2008. PLoS One 3(9):e3257*
A	GTGGCTTTGGAGTTGCAGTT	-	*Antes et al. 2011. NAR 38(19):6466-6476*
B1	-	CAGCCACCATGAATATTGTAC	*Antes et al. 2011. NAR 38(19):6466-6476*
B2	-	GAAGCAGATTTGGGTACCAC	*Antes et al. 2011. NAR 38(19):6466-6476*

Table S1. RT-qPCR and qPCR primers. The sequence of forward and reverse primers for RT-qPCR (upper panel) and qPCR (lower panel) is indicated after the name of the probe that also indicats the gene analysed. Number in parenthesis indicate different sets used to test the same gene. The pair A-B1 amplifies a mtDNA region included in 7S, while the pair A-B2 amplifies a region beyond 7S in the direction of the H-strand (see scheme in Supplementary Figure S6D). Reference is indicated in the last column.

Probe	start	end	size
14-1	650	1598	949
ND1	3515	3715	200
ATP8	8366	8566	200

mTOTΔr	probes 3 to 13 (rRNA probes excluded)

Table S2. Coordinates of additional probes used in this study. The start and end points of probes used for FISH experiments are given on the mitochondrial DNA (NC_012920, GenBank). mTOTΔr, which is a mix of eleven probes is indicated below.